Loss of material trainability through an unusual transition

Himangsu Bhaumik and Daniel Hexner *

Faculty of Mechanical Engineering, Technion, 320000 Haifa, Israel

Material training is a method to endow materials with specific responses through external driving. We study the complexity of attainable responses, as expressed in the number of sites that are simultaneously controlled. With increased complexity, convergence to the desired response becomes very slow. The training error decays as a power law with an exponent that varies continuously and vanishes at a critical threshold, marking the limit of trainable responses. We study how the transition affects the vibrational properties. Approaching the critical threshold, low-frequency modes proliferate, approaching zero frequency. This implies that training causes material degradation and that training fails due to competing spurious low-frequency modes. We propose that the excess low-frequency spectrum is due to atypical local structures with bonds that nearly align. Our work explains how the presence of an exotic critical point affects the convergence of training, and could be relevant for understanding learning in physical systems.

Introduction. Networks are a common representation of natural and engineered systems that process high-dimensional set of inputs [1]. These include natural and synthetic neural networks [2–4] that perform computations or store memories [5], regulatory networks [6], and more recently, elastic and flow networks that encode complex responses [7–11]. A central challenge in these systems is understanding the capacity of such networks, in terms of the complexity of the responses that can be attained. It is not surprising that as the difficulty of the response is increased, the system fails to yield the desired behavior. These limitations can be either attributed to the capacity of the network itself or the algorithm by which the parameters are adjusted [12].

In this Letter we consider the capacity of mechanical networks that are trained through sequences of applied strains. We build on recent work that demonstrated that disordered networks can be trained with externally applied fields [11,13]. During the training the external driving generates stresses which cause the network to remodel its structure through plastic deformations. As a result the system evolves to yield the desired response. Training can be considered a learning process, where the material itself learns without the use of a computer [14–17]. In contrast to designed structures, this approach does not require fabrication, nor manipulating directly the microscopic structure, and is therefore potentially scalable.

We focus on the convergence of the response as a function of the number of target sites that are simultaneously controlled. As the number of target sites is increased,

*danielhe@me.technion.ac.il

training becomes very sluggish. The training error decays approximately as a power law with an exponent that varies continuously with the number of trained sites. At a critical threshold the exponent appears to vanish, indicating a phase transition. Unlike conventional critical points, here, power laws are observed over a broad range of parameters [18–22]. The transition also marks the limits of attainable responses. We find that the capacity, defined by the number of sites that can be simultaneously controlled, is approximately extensive, scaling with system size.

We conclude by searching for a signature of this transition in the vibrational properties. We find a substantial increase in the low-frequency spectrum as complexity is increased. The trained response can be associated with a single low-frequency mode that is separated from the remainder of the spectrum [23]. Here, failure is accompanied with a proliferation of low-frequency modes that compete with the desired response. At criticality the density of states appears to creep down to arbitrarily small frequencies. We provide evidence that the excess low-frequency modes are due to nongeneric geometries, characterized by bonds that align.

Model. We employ the model and training protocol of Ref. [11], which is briefly summarized. We model an amorphous material as a network of springs in two dimensions. The force on each spring is given by $k_i(\ell_i - \ell_{i,0})$, where ℓ_i is the length of the bond, $\ell_{i,0}$ the rest length, and k_i is the spring constant. For convenience we consider networks that are derived from the amorphous packing of repulsive spheres at zero temperature. The networks are characterized by their coordination number $Z = \frac{2N_b}{N}$, where N_b is the number of bonds and N is the number of nodes. Rigidity requires that $Z > Z_c \simeq 2d$ [24–27].

Our goal is to train responses where a single input strain at a source site yields a prescribed strain on N_T randomly chosen target sites, as illustrated in Fig. 1. Each source and target site is pairs of nearby nodes and the local strain is defined as the fractional change in their distance. We denote that strain on
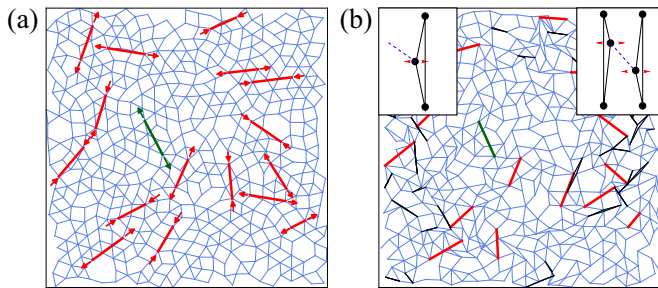
FIG. 1. An example of (a) an initial network and (b) a trained network (with $N = 500$ nodes). Each pair of source sites and target sites is marked by a connecting green and red line, respectively. The response of the targets can either be in phase or out of phase with respect to the source, as indicated by the arrows. In the trained network the angles between adjacent bonds may become small (bonds with $\theta < 10°$ are drawn in black). The left inset shows a structural motif which has a soft direction (marked in red) when detached from the network by cutting the blue bond. The right inset shows two coupled motifs that contribute to localized low-frequency modes.

the source and target by ϵ_S and ϵ_T. The strain on both the source and targets is chosen to have the same amplitude, ϵ_{Age}, however, the response is chosen to be in phase or out of phase with equal probability.

Training relies on plastic deformations that alter the structure of the network. Here, we only consider changes to the rest lengths [28]. Each bond is modeled as a Maxwell viscoelastic element [29], where the change in the rest length is proportional to the force on the bond,

$$\partial_t \ell_{i,0} \propto k_i(\ell_i - \ell_{i,0}). \tag{1}$$

We focus on the quasistatic regime, where the time to reach force balance is small with respect to the timescales of plasticity. In simulations time is discretized into small steps, where at each step, we vary the strain, minimize the energy to reach force balance, and then evolve the rest length in accordance with Eq. (1).

The response of an elastic network is dominated by the softest direction in the energy landscape, and therefore we aim at sculpting an energy "valley" that couples the input source site and an output target site. In our model, the rest lengths evolve to lower the internal stresses and elastic energy. Training an energy valley is therefore performed by cyclically straining the source and targets along the desired response, while allowing plastic deformation to sculpt the energy landscape. The source and target sites are strained by attaching the pairs of nodes with "ghost bonds" and varying their rest length.

Convergence and phase transition. To test the generality of our results we consider both small and large $\Delta Z \equiv Z - Z_c$, with corresponding values of $\Delta Z \approx 0.03$ and $\Delta Z \approx 0.75$, respectively. In the small ΔZ limit the networks are nearly isostatic, and elasticity is anomalously long ranged [30,31]. The long-range response to pinching a bond has been shown to be useful in coupling distant sites during training [11]. Therefore, for large ΔZ training is only successful for a sufficient number of targets [11]. Nonetheless, we find that the qualitative results are similar.
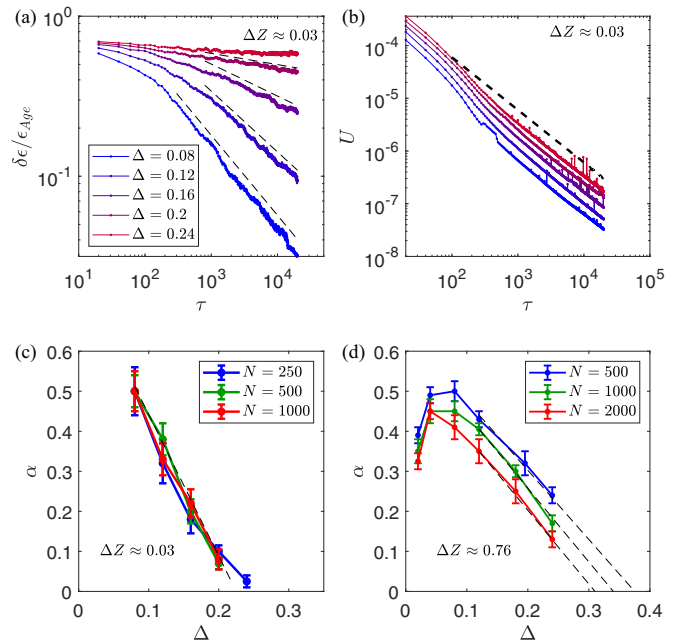

FIG. 2. Characterizing convergence as a function of the number of targets per node, $\Delta = N_T/N$. (a) The training error as a function of the number of cycles. With increased Δ, convergence becomes very slow, decaying approximately as a power law. The dashed lines are a guide to the eye. (b) The decrease in energy along the training path is weakly dependent on N_T. The exponent α as a function of Δ for small (c) and large (d) coordination number. α appears to vanish at a critical threshold that depends weakly on N. In (a) and (b), $N = 500$.

We characterize the convergence of the response by measuring the error $\delta\epsilon$, defined as the difference in the absolute value from the desired response. We average the error over an entire cycle, where the strain is varied up to ϵ_{Age}, and over the number of targets. Figure 2(a) shows $\delta\epsilon/\epsilon_{Age}$ as a function of the number of training cycles for different numbers of target sites N_T, as conveniently indicated by $\Delta \equiv \frac{N_T}{N}$. As Δ increases the convergence becomes slower and slower. At long times $\delta\epsilon$ decays approximately as a power law,

$$\delta\epsilon \propto \tau^{-\alpha}. \tag{2}$$

Figure 2(c) shows that α depends on Δ; it decreases with Δ and appears to vanish at a finite value Δ_c. Exploring the regime near Δ_c is unavoidably difficult due to the slow convergence rate.

We interpret the point $\Delta = \Delta_c$ as a critical point separating converging responses, from unattainable responses. This transition is unlike conventional continuous phase transitions where power-law scaling occurs only at the critical point. Here, over the entire range of $\Delta < \Delta_c$ convergence scales as a power law, which implies extremely slow convergence. Assuming we are satisfied with an error, $\delta\epsilon_m$, the time required scales as $\tau \propto (\delta\epsilon_m)^{-1/\alpha}$. Taking $\alpha \propto |\Delta - \Delta_c|^{\beta \approx 1}$ yields a Vogel-Fulcher-Tammann-like law [32–34] $\tau \propto e^{A|\Delta - \Delta_c|^{-\beta}}$, where $A = -\log\epsilon_m$. This is far slower than the power-law divergence in conventional phase transitions $\tau \propto |\Delta - \Delta_c|^{-\theta}$.

We note that similar behavior has been observed in another class of nonequilibrium phase transitions, that separates

a static absorbing phase from a chaotic phase [35,36]. The directed percolation class has the characteristics of a critical transition with power-law scalings, however, when quenched disordered is added the nature of the transition changes and there is a regime where activity decays as a power law with a continuously varying exponent [18–22]. The effect where disorder alters the pristine transition is known as a Griffiths phase. The origin of this behavior can be traced to rare regions that have an overwhelming contribution.

In our system, there is also a convergence to absorbing states. Training reduces the energy along a prescribed path until the energy vanishes. At that point, when there are no longer any internal forces, the system ceases to evolve, thus reaching an absorbing state. However, in contrast to the strong dependence of the error on Δ, the decay of the elastic energy shown in Fig. 2(b) is nearly independent of Δ and is relatively quick, scaling approximately as τ^{-1}. This suggests that regardless of Δ the evolution of the networks slows down and ultimately freezes.

Capacity. Next, we consider the system size dependence. Figure 2(c) shows that for small ΔZ the exponent α is very weakly dependent on system size. This suggests that Δ_c is approximately constant, implying the number of sites that can be simultaneously trained is extensive, proportional to N. Figure 2(d) shows α as a function of Δ for systems with large ΔZ and for different system sizes. The exponent α is maximal at an intermediate value of Δ; there, it depends weakly on system size. We estimate $\Delta_c(N)$ by extrapolating to the point where α vanishes and find that it slightly decreases with N. Over a fourfold increase in system size, Δ_c changes only by approximately 13%. Thus, capacity is nearly extensive. Despite this slight decrease of capacity with system size, the large ΔZ networks have a larger Δ_c than of the small ΔZ networks.

We note that the (near) extensive capacity is different than the subextensive scaling found in tuning networks by bond removal and addition in Ref. [10].

Lastly, we note that there is an additional system dependent timescale (see Sec. S4 in the Supplemental Material [37]), which marks the crossover to the power-law regime. We find that this timescale grows approximately as $N^{\approx 0.6}$, implying that larger systems take longer time to train (see Sec. S4 in the Supplemental Material [37]). We rationalize this timescale by noting that training is only successful when the stiffness along the training path falls below the remaining transverse stiffnesses, which are defined by the system's eigenfrequencies. The lowest frequency in the system on average decreases with system size and therefore larger systems require more training to further reduce the stiffness along the trained path.

Normal mode analysis. As noted, the response depends on the ratio of the stiffness in the transverse directions to the stiffness along the trained path. Since the decay of energy in Fig. 2(b) weakly depends on Δ, this suggests that transverse stiffness becomes small. Within linear response, the stiffness corresponds to the eigenfrequencies, which are characterized by the density of states. To this end, we compute the Hessian H, defined by the matrix of second derivatives of the energy, and diagonalize it to find its spectrum. Previously it was found that the lowest mode corresponds to the trained response [23],
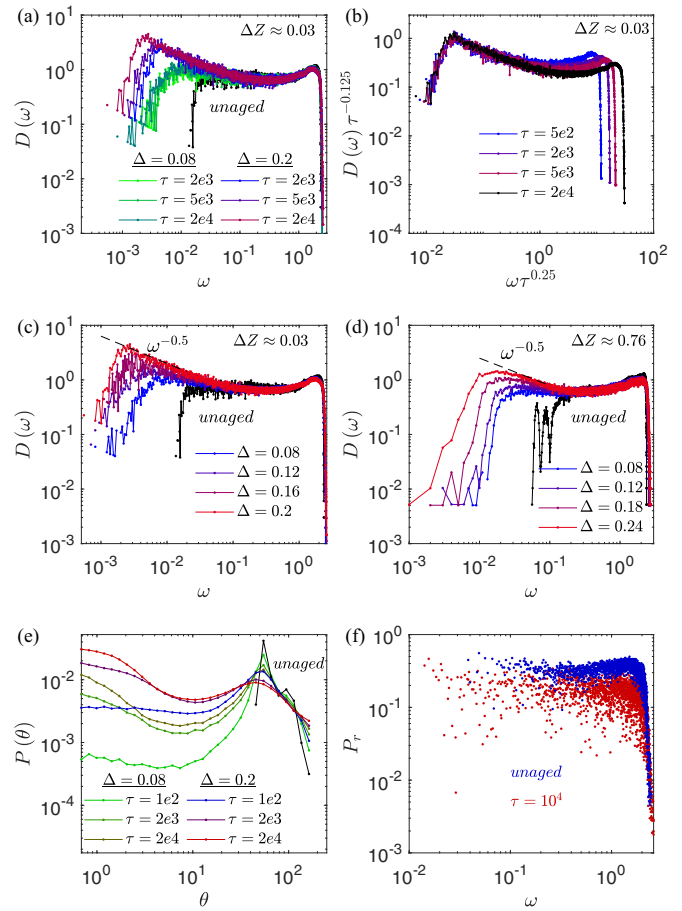

FIG. 3. Characterization of the vibrational properties. (a) The evolution of the density of states with the number of cycles. For small Δ the density of states ceases to evolve after $\tau \sim 200$ cycles, while for larger Δ it continuously shifts to lower frequencies with additional training. (b) A collapse of the density of states near the transition ($\Delta = 0.2$) suggests that the shift to lower frequencies scales as $\omega_c \propto \tau^{-0.25}$. (c) and (d) The density of states at a fixed number of cycles, $\tau = 2 \times 10^4$ for different values of Δ. In (c), $\Delta Z \approx 0.03$, while in (d), $\Delta Z \approx 0.76$. In both cases the shift to lower frequencies grows with Δ. (e) The distribution of the angles (measured in degrees) between bonds for different numbers of cycles. (f) The participation ratio before training (blue) and after 10^4 training cycles (red). In (e) and (f), $N = 1000$, $\Delta Z \approx 0.76$.

and therefore the remaining frequencies correspond to the transverse stiffnesses.

Prior to training there are very few modes below a characteristic frequency, $\omega^* \propto \Delta Z$ [38]. Figure 3(a) shows the evolution of the density of states $D(\omega)$ for two values of Δ. For clarity, we exclude the lowest-frequency mode associated with the trained response. We observe two behaviors depending on the distance to Δ_c. Near Δ_c there is a continual shift towards lower frequencies with the number of cycles, whereas away from Δ_c the density of states is nearly stationary after about ~ 200 cycles. To probe the evolution of the density of states near the transition we collapse the curves at low frequencies. Figure 3(b) shows that the shift to lower frequencies scales approximately as $\tau^{-0.25}$, suggesting a continual shift to

zero frequency. This feature is not present in previously found Griffiths phases.

Next, we study the dependence of the density of states on Δ at fixed τ. Figures 3(c) and 3(d) show the density of states for small and large ΔZ correspondingly. In both cases, as Δ increases there is a shift towards lower frequencies. The trend is suggestive that asymptotically, at Δ_c the density of states extends to zero frequency. At small frequencies, $D(\omega)$ can be fitted by $\omega^{-0.5}$.

The enhanced low-frequency spectrum explains how training fails. As noted, the response is governed by the ratio of the stiffness along the trained direction and the transverse stiffnesses. The proliferation of low-frequency modes indicates that there are many competing spurious modes. Therefore, more training cycles are needed to decrease the stiffness along the training path. In the Supplemental Material [37] we show the error scales as the ratio of the two lowest frequencies squared. We also note that retraining a material repeatedly also results in an excess in the low-frequency spectrum [23].

Structural features and nature of low-frequency modes. Next, we search for the origin of the excess low-frequency modes in the structure. Figure 1 shows the network before [Fig. 1(a)] and after training [Fig. 1(b)]. In the trained network some of the angles between bonds becomes very small. Prior to training the smallest angle formed by adjacent bonds is $\theta \approx 39°$. As shown in Fig. 3(e) the distribution at a small angle becomes pronounced with increased training, especially for large Δ. To relate the small angles to the low-frequency modes, we note that an unstressed bond assigns an energy cost for node displacements that alter the bond's length. This can be considered a constraint on the zero-energy motions. When two bonds align ($\theta = 0, \pi$) these two constraints are redundant, reducing the stiffness along the transverse direction.

We have identified local structural motifs where bond alignment leads to soft deformations. We illustrate this in the example shown in the inset of Fig. 1(b) (left). In the absence of the bond by which the motif is attached to the network (marked in blue) the transverse motion is soft, but constrained when the bond is present. However, two motifs can couple [see the inset of Fig. 1(b) (right)] to form a soft energy deformation. If the bonds in the motifs perfectly align this leads to a local zero mode. The motif where all the bonds of a given node align yields a soft deformation, however, this motif is rare. Thus, through individual and coupled motifs the eigenfrequencies are shifted to lower values.

We also characterize the low-frequency modes by computing the participation ratio P_r (see Sec. S5 in the Supplemental Material [37]). As shown in Fig. 3(f), P_r of the trained network decreases over the whole frequency range. We associate the increased localization with local soft motifs. In addition, and

similarly to the untrained network, there are also extended modes. An additional discussion on the soft motifs and normal modes is provided in the Supplemental Material [37].

We consider the enhancement of the low-frequency spectrum as degradation. The shift towards lower frequencies implies that there is an overall softening of the system. In the Supplemental Material [37] we show that both the bulk and shear modulus decrease with the number of training cycles, in particular near Δ_c. We therefore believe that this transition could be of interest in studying aging under a periodic drive (or material fatigue).

Conclusions. In summary, we have studied the effect of varying the complexity of the trained responses. The most prominent behavior is that convergence becomes very slow with increasing difficulty, manifesting through a power-law decay of the error. At a critical threshold the exponent vanishes, implying that the convergence time diverges with a Vogel-Fulcher-Tammann-like law. At small ΔZ we find that the critical threshold Δ_c is independent of system size, implying that responses with an extensive number of sites can be trained. At larger connectivity the capacity appears nearly extensive, with a weak system size dependence.

To characterize the transition we also studied the density of states and the normal modes. With increased difficulty, the density of states creeps towards lower frequencies. Near the transition it appears that the low-frequency modes reach arbitrarily small frequencies with sufficient training. We show that the growing number of lower-energy modes compete with the desired response. The system cannot distinguish between the trained response and the spurious low-energy modes. We have also studied the structural source of the low-frequency modes and characterized the eigenmodes.

Our work demonstrates how an exotic critical point affects training. The nearness to the critical point defines a difficulty measure, and while we have focused on the number of targets, the difficulty of the trained response could have other contributions, including the nonlinearity of the response [39] or its strain amplitude. With increased difficulty, there is also an increase in degradation, marked by the enhanced low-frequency spectrum. This could affect the robustness of the response as well as the number of times the system can be retrained [23]. It is interesting to question the universality of this type of transition, and whether it applies to other forms of training. In particular, since training is intimately related to learning [14–17], perhaps a similar transition occurs in other learning algorithms.

[1] B. Barzel and A.-L. Barabási, Universality in network dynamics, Nat. Phys. **9**, 673 (2013).

[2] D. S. Bassett and O. Sporns, Network neuroscience, Nat. Neurosci. **20**, 353 (2017).

[3] S. B. Kotsiantis, Supervised machine learning: A review of classification techniques, in *Emerging Artificial Intelligence*

Applications in Computer Engineering, edited by I. Maglogiannis, K. Karpouzis, B. A. Wallace, and J. Soldatos, Frontiers in Artificial Intelligence and Applications (IOS Press, Amsterdam, 2007), Vol. 160 , p. 3.

[4] P. Mehta, M. Bukov, C.-H. Wang, A. G. Day, C. Richardson, C. K. Fisher, and D. J. Schwab, A high-bias, low-variance

introduction to machine learning for physicists, Phys. Rep. **810**, 1 (2019).

[5] J. J. Hopfield, Neural networks and physical systems with emergent collective computational abilities, Proc. Natl. Acad. Sci. USA **79**, 2554 (1982).

[6] E. H. Davidson, *The Regulatory Genome: Gene Regulatory Networks in Development and Evolution* (Elsevier, Amsterdam, 2010).

[7] M. R. Mitchell, T. Tlusty, and S. Leibler, Strain analysis of protein structures and low dimensionality of mechanical allosteric couplings, Proc. Natl. Acad. Sci. USA **113**, E5847 (2016).

[8] J. W. Rocks, N. Pashine, I. Bischofberger, C. P. Goodrich, A. J. Liu, and S. R. Nagel, Designing allostery-inspired response in mechanical networks, Proc. Natl. Acad. Sci. USA **114**, 2520 (2017).

[9] L. Yan, R. Ravasio, C. Brito, and M. Wyart, Architecture and coevolution of allosteric materials, Proc. Natl. Acad. Sci. USA **114**, 2526 (2017).

[10] J. W. Rocks, H. Ronellenfitsch, A. J. Liu, S. R. Nagel, and E. Katifori, Limits of multifunctionality in tunable networks, Proc. Natl. Acad. Sci. USA **116**, 2506 (2019).

[11] D. Hexner, A. J. Liu, and S. R. Nagel, Periodic training of creeping solids, Proc. Natl. Acad. Sci. USA **117**, 31690 (2020).

[12] T. Schoning, A probabilistic algorithm for k-SAT and constraint satisfaction problems, in *40th Annual Symposium on Foundations of Computer Science (Cat. No. 99CB37039)* (IEEE, New York, 1999), pp. 410–414.

[13] N. Pashine, D. Hexner, A. J. Liu, and S. R. Nagel, Directed aging, memory, and nature's greed, Sci. Adv. **5**, eaax4215 (2019).

[14] B. Scellier and Y. Bengio, Equilibrium propagation: Bridging the gap between energy-based models and backpropagation, Front. Comput. Neurosci. **11**, 24 (2017).

[15] M. Stern, C. Arinze, L. Perez, S. E. Palmer, and A. Murugan, Supervised learning through physical changes in a mechanical system, Proc. Natl. Acad. Sci. USA **117**, 14843 (2020).

[16] J. Kendall, R. Pantone, K. Manickavasagam, Y. Bengio, and B. Scellier, Training end-to-end analog neural networks with equilibrium propagation, arXiv:2006.01981.

[17] M. Stern, D. Hexner, J. W. Rocks, and A. J. Liu, Supervised Learning in Physical Networks: From Machine Learning to Learning Machines, Phys. Rev. X **11**, 021045 (2021).

[18] A. J. Noest, New Universality for Spatially Disordered Cellular Automata and Directed Percolation, Phys. Rev. Lett. **57**, 90 (1986).

[19] A. G. Moreira and R. Dickman, Critical dynamics of the contact process with quenched disorder, Phys. Rev. E **54**, R3090 (1996).

[20] H. K. Janssen, Renormalized field theory of the Gribov process with quenched disorder, Phys. Rev. E **55**, 6253 (1997).

[21] R. Dickman and A. G. Moreira, Violation of scaling in the contact process with quenched disorder, Phys. Rev. E **57**, 1263 (1998).

[22] T. Vojta, Rare region effects at classical, quantum and nonequilibrium phase transitions, J. Phys. A: Math. Gen. **39**, R143 (2006).

[23] D. Hexner, Adaptable materials via retraining, arXiv:2103.08235.

[24] J. C. Maxwell, L. On the calculation of the equilibrium and stiffness of frames, London, Edinburgh, Dublin Philos. Mag. J. Sci. **27**, 294 (1864).

[25] C. Calladine, Buckminster Fuller's "'Tensegrity" structures and Clerk Maxwell's rules for the construction of stiff frames, Int. J. Solids Struct. **14**, 161 (1978).

[26] S. Pellegrino, Structural computations with the singular value decomposition of the equilibrium matrix, Int. J. Solids Struct. **30**, 3025 (1993).

[27] S. Alexander, Amorphous solids: Their structure, lattice dynamics and elasticity, Phys. Rep. **296**, 65 (1998).

[28] D. Hexner, N. Pashine, A. J. Liu, and S. R. Nagel, Effect of directed aging on nonlinear elasticity and memory formation in a material, Phys. Rev. Res. **2**, 043231 (2020).

[29] J. C. Maxwell, IV. On the dynamical theory of gases, Philos. Trans. R. Soc. London **157**, 49 (1867).

[30] W. G. Ellenbroek, E. Somfai, M. van Hecke, and W. van Saarloos, Critical Scaling in Linear Response of Frictionless Granular Packings near Jamming, Phys. Rev. Lett. **97**, 258001 (2006).

[31] E. Lerner, E. DeGiuli, G. Düring, and M. Wyart, Breakdown of continuum elasticity in amorphous solids, Soft Matter **10**, 5085 (2014).

[32] H. Vogel, Das Temperaturabhaengigkeitsgesetz der Viskositaet von Fluessigkeiten, Phys. Z. **22**, 645 (1921).

[33] G. S. Fulcher, Analysis of recent measurements of the viscosity of glasses, J. Am. Ceram. Soc. **8**, 339 (1925).

[34] G. Tammann and W. Hesse, Die abhängigkeit der viscosität von der temperatur bie unterkühlten flüssigkeiten, Z. Anorg. Allg. Chem. **156**, 245 (1926).

[35] P. Grassberger and A. de la Torre, Reggeon field theory (Schlögl's first model) on a lattice: Monte Carlo calculations of critical behaviour, Ann. Phys. **122**, 373 (1979).

[36] H. Hinrichsen, Non-equilibrium critical phenomena and phase transitions into absorbing states, Adv. Phys. **49**, 815 (2000).

[37] See Supplemental Material at http://link.aps.org/supplemental/10.1103/PhysRevResearch.4.L042044 for additional data on the generality of the results, degradation, and system size time scale.

[38] C. S. O'Hern, L. E. Silbert, A. J. Liu, and S. R. Nagel, Jamming at zero temperature and zero applied stress: The epitome of disorder, Phys. Rev. E **68**, 011306 (2003).

[39] D. Hexner, Training nonlinear elastic functions: Nonmonotonic, sequence dependent and bifurcating, Soft Matter **17**, 4407 (2021).